ORIGINAL ARTICLE

CIWEM Chartered Institution of Water and Environmental Management   Journal of Flood Risk Management   WILEY

Determining the vehicle instability risk in stream crossings

Ricardo A. Bocanegra [ORCID] | **Félix Francés** [ORCID]

Research Institute of Water and Environmental Engineering (IIAMA), Universitat Politècnica de València, Valencia, Spain

Correspondence
Ricardo A. Bocanegra, Research Institute of Water and Environmental Engineering (IIAMA), Universitat Politècnica de València, Cami de Vera 0, Valencia 46017, Spain.
Email: ribovi@doctor.upv.es

Abstract

Floods negatively affect roads, vehicles and transport systems in general. The impact on these systems leads to a cascasing effect with significant repercussions. Due to this, the evaluation of the instability risk to which the vehicles are subjected in stream crossing is necessary for the integral management of floods. A methodology was herein developed that allows instability risks due to floods to be estimated for vehicles driving through stream crossings, which may correspond to fords, vented fords or bridges. Risk was calculated by combining hazard and vulnerability. To determine hazard, a stability function of partially submerged vehicles, the geometric characteristics of vehicles, the hydrodynamic characteristics of floods (water depths and velocities) and the probability of them occurring were employed. Vulnerability was determined by combining exposure and susceptibility, which are respectively established with the exposure and damage function. To determine exposure, a limit water depth to interrupt the traffic of vehicles through the flooded area was considered. The developed methodology was applied to the Godelleta municipality (Spain), and found that roughly one quarter of the stream crossings in this study area presented a relatively high vehicle instability risk due to floods because it exceeded 0.2 vehicles/year.

KEYWORDS

floods, limit water depth, stream crossings, vehicle instability risk, vehicle stability

1 | INTRODUCTION

Floods are a natural phenomenon with major negative impacts on society because they cause substantial indirect and direct losses that affect people's lives and health, deteriorate existing infrastructures and interrupt different public services and productive activities (Yin et al., 2016). Those elements and activities that floods affect include roads, vehicles and transport systems in general. The impact on these systems leads to a cascasing effect with possible local and/or regional repercussions (Suárez et al., 2005).

Floods are the main reason for interrupting public and private transport systems (Pregnolato et al., 2017), and this is expected to continue in the future (Dawson et al., 2016). Moreover, the effects of floods on cars and transport systems may worsen due to roads themselves because a road network can modify the natural topography and create a new drainage network, which can change the hydrological response of basins (Jones et al., 2000; Wemple et al., 2001).

Several studies have pointed out that many people die when attempting to cross flooded areas in their vehicles (Drobot et al., 2007; Fitzgerald et al., 2010). In 1989, a

flood that took place in the city of Nagasaki, Japan, damaged 20,000 cars and 299 people died, of whom roughly 20 died when their vehicles were dragged away by overflowing flood water (Ishikawa & Komatsu, 2014). In September 2019, rainfall exceeding 400 mm in 48 h fell in SE Spain. Seven people were killed, of whom four were trapped in their cars and died (Levanter, 2019). In Brazil, extremely heavy rainfall in January 2020 and at least 53 people died, and several people did so inside their vehicles (Foal de S. Paulo, 2020).

Despite the negative impact of floods, and the fact that the integral management of such events requires assessing the risk posed for vehicles, very few studies have centred on determining the negative effects of floods on transport systems (Malarias et al., 2014). The Word Group (Prada & Carolina, 2015) presented a simple equation to calculate risks on road networks owing to floods. In this equation, risk is expressed as either number of deaths per year or economic cost per year, which is obtained with the summation of the product of the following factors: (i) hazardousness, understood as the probability of a threatening event happening; (ii) exposure, understood as the probability of vehicles being affected by the threatening event; (iii) vulnerability, which ranges between 0 and 1, and indicates the severity of the expected damage; and (iv) total potential loss, which is expressed as the number of people who died or economic costs.

Of the few studies that have centred on studying risk components specifically in stream crossings, we find that presented by Michielsen et al. (2016) and Kalantari et al. (2019). Based on the analysis of the physical basin characteristics and by implementing statistical methods, in both cases, authors developed a methodology that could predict if stream crossings in a given area are prone to flooding.

A methodology was herein developed that allows the vehicle instability risk to be estimated. This risk is posed by the growing river levels for vehicles when they cross stream crossings, which may correspond to fords, vented fords and bridges. We stress that this methodology can be used on bridges whose decks might be flooded, and whose structures would not hypothetically fail structurally during flooding.

Our article firstly presents a brief description of the mechanisms that lead to loss of vehicle stability. Then it describes the methodology developed to obtain the instability risk posed for those vehicles driving through a stream crossing. This risk is calculated by the discrete solution of the statistical integral of the product of hazard by vulnerability, which is a more elaborate calculation that those presented in former studies. Next it implements this methodology in the Godelleta municipality

(Spain), where 32 stream crossings are identified. Finally, it offers the main conclusions drawn from developing and implementing the proposed methodology.

2 | STABILITY OF PARTIALLY SUBMERGED VEHICLES

2.1 | Partially submerged vehicles' loss of stability

Loss of vehicle stability in flooded areas can be caused by three kinds of hydrodynamic mechanisms: floating, sliding and toppling. The floating phenomenon occurs when the floating and lift forces caused by flow exceed a vehicle's weight. This mechanism occurs mainly when flowing water moves quite slowly and over considerable depths (Sand et al., 2011).

Sliding happens when the drag force caused by flow exceeds the friction force, which depends on the vehicle's weight and on the friction between vehicle's wheels and the road surface. Floating and sliding mechanisms interact because the floating and lift forces diminish the normal weight component, by means of which the friction force lowers and vehicles can be dragged even when depths are not so great (Arrighi et al., 2015).

The toppling mechanism apparently takes place having lost vehicle stability due to floating or sliding mechanisms on irregular land (Shand et al., 2011). To date, this mechanism has not been studied in-depth.

2.2 | Vehicle instability index

According to Bocanegra and Francés (2021), the flood hazard for vehicles corresponds to the probability of overflowing water unstabilising cars. In the methodology herein presented, vehicle stability is defined with the criterion proposed by Arrighi et al. (2016) because it is one of the most robust available methods (Bocanegra et al., 2020).

In the method proposed by Arrighi et al. (2016), the stability of a vehicle type i is established with a vehicle instability index, S_i, which is defined as the relation between a critical mobility parameter θv_{cr} and a mobility parameter θv_i defined for the reference vehicle. These parameters are calculated with the equations below:

$$\theta_{Vcr} = 8.2\,Fr^2 - 14.1\,Fr + 5,4 \tag{1}$$

$$\theta_{v_i} = \frac{2L}{(H_v - h_c)}\frac{l}{l\,Cos\beta + L\sin\beta}\left(\frac{\rho_c\,(H_v - h_c)}{\rho\,(H - h_c)} - 1\right) \tag{2}$$

where Fr is the Froude number, ρ_c is the car's mean density, ρ is water density, h_c is the distance between the chassis and the ground, H is the undisturbed water depth, β is the angle of flow incidence, and H_v, L and l are car height, car length and car width, respectively.

In mathematical terms, the stability of vehicle i is established with this expression:

$$S_i = \frac{\theta_{Vcr}}{\theta_{Vi}} \begin{cases} \geq 1 & \text{Vehicle moves due to sliding} \\ < 1 \text{ and} \geq 0 & \text{Stationary vehicle} \\ < 0 & \text{Vehicle moves due to floating} \end{cases} \quad (3)$$

3 | METHODOLOGY

The vehicle instability risk due to floods in stream crossings (R) corresponds to the annual mean number of vehicles whose stability would be lost when crossing these places. According to Bocanegra and Francés (2021), this risk can be calculated with the expression below:

$$R_i = \int_0^1 V(s_i)\, dF_{s_i} = \int_0^\infty V_i(s) f_{s_i}(s)\, ds \quad (4)$$

where R_i is the vehicle instability risk for vehicles type i, $V(s_i)$ is vulnerability, F_{Si} is the distribution function of the accumulated probability of S_i and f_{Si} is the probability density function.

The procedure that must be followed to calculate the hazard, vulnerability and, finally, the instability risk of vehicles in stream crossings, is presented below.

3.1 | Vehicle instability hazard

The flood hazard for vehicle i in a stream crossing is obtained by combining the probability of a flooding event taking place with the values that the vehicle instability index, S_i, would take. The details to obtain the hazard are found in Bocanegra and Francés (2021) for a flooding zone where there are flooding maps for different return periods.

The scheme in Figure 1 shows a diagram of the procedure to calculating this hazard for a type i vehicle at a given stream crossing. On the one hand, panel A of this figure represents the probability of occurrence of each flood against the parameters through which its magnitude is established (depth and velocity). On the other hand, each flood event corresponds to a vehicle instability index, S_i, which is calculated by Equation (3); panel B of Figure 1 relates the magnitude of each flood with its corresponding value of S_i. Finally, combining these two results, the instability hazard is obtained as the
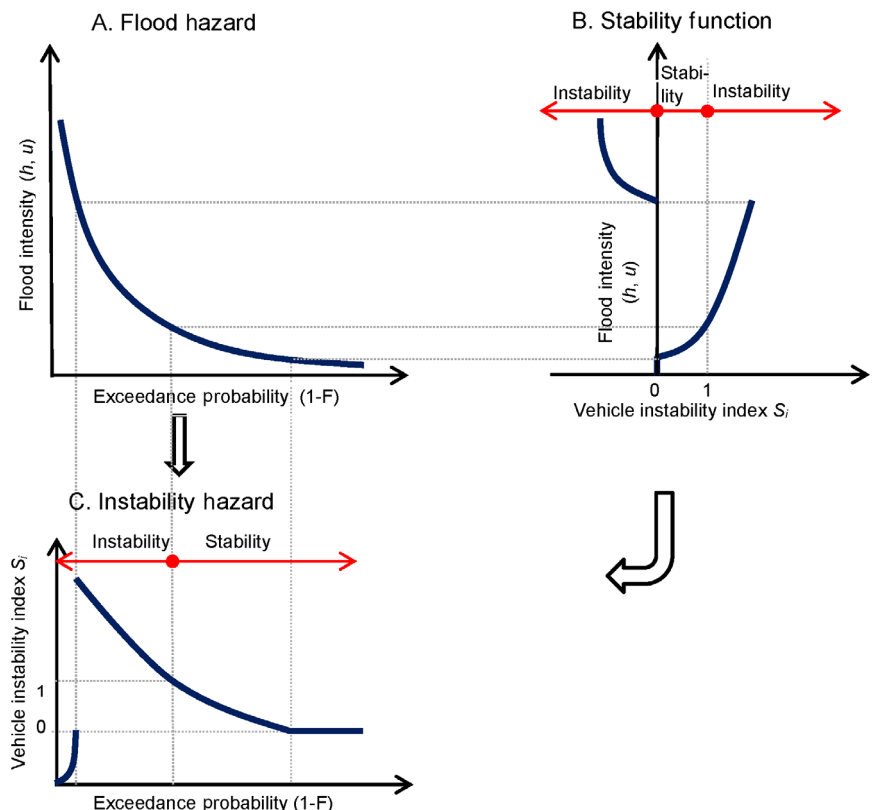

FIGURE 1 Outline of the process to follow to calculate the instability hazard in one vehicle i in a stream crossing. Source: Bocanegra and Francés (2021)
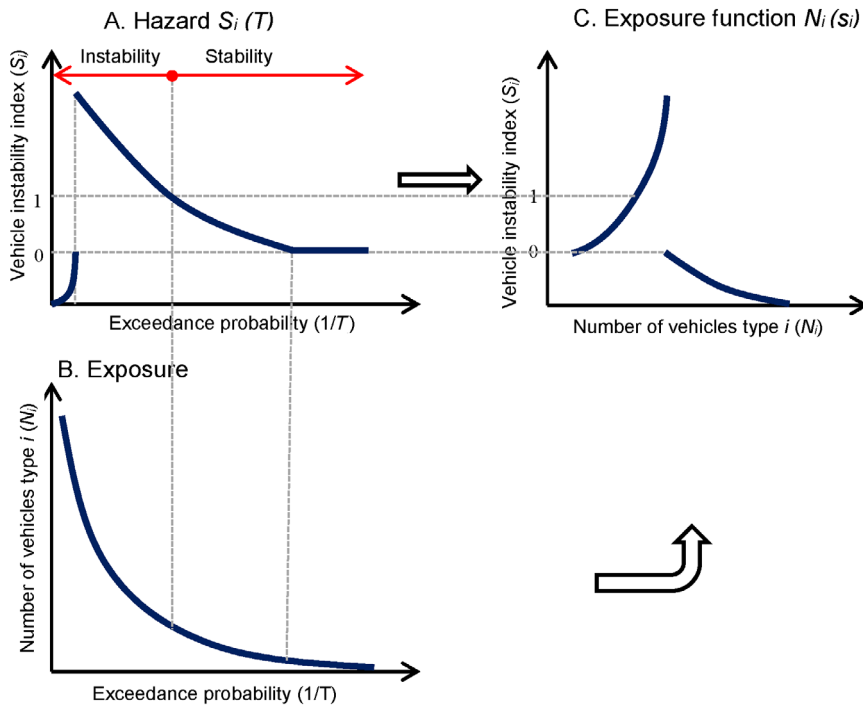
FIGURE 2   Outline of the process to determine the exposure function of vehicles type i
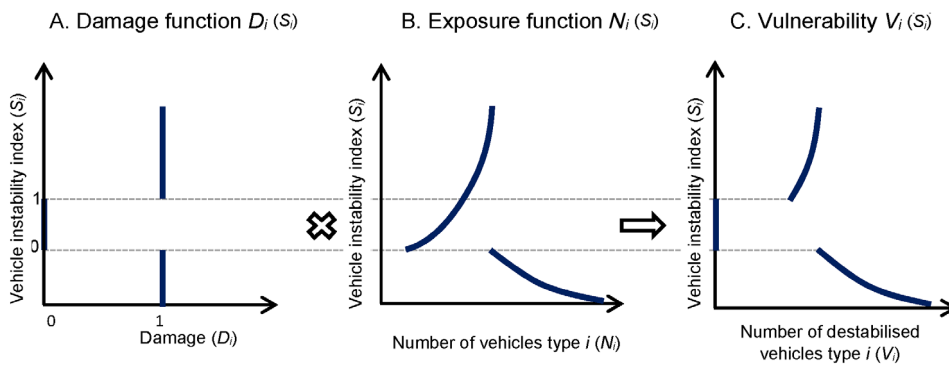

FIGURE 3   Outline of the procedure to obtain vulnerability of vehicles type i in the event of floods

probability of occurrence of each event of flood against its respective value of S_i, as presented in panel C of this figure.

With stream crossings, it is sufficient to employ the maximum annual flow quantiles for a set of return periods and to convert this discharge into water depths and velocities by a 1D hydraulic stationary model with an adequate flow hypothesis (critical flow, uniform flow, etc.).

3.2 | Vulnerability

Vulnerability corresponds to a system's characteristics that make it susceptible to suffer damage by a threat (UNISDR, 2009). Vulnerability depends on the degree of the elements that can be affected by flooding from being exposed, and by their susceptibility. This susceptibility

indicates the degree of damage that these elements can suffer and is normally expressed by damage or loss functions.

3.2.1 | Exposure

In the problem being solved, exposure was the number of each vehicle type i that could cross stream crossings while water levels rose. Since the duration of the flood increases as its return period T increases, the number of potentially affected vehicles type i. N_i will depend on the return period and can be denoted as $N_i(T)$ and schematized in Figure 3, panel B. This exposure can be estimated as follows.

If the vehicle traffic distribution in time was the Poisson type, which has been applied to low and medium vehicle flows (Cal y Mayor & Cárdenas, 2007), it is

possible to demonstrate that the number of vehicles, $N_i(T)$, corresponds to the following expression:

$$N_i(T) = q\, g_i \Delta t_i(T) \qquad (5)$$

where q corresponds to the vehicle type i traffic in the stream crossing during a flood. If no further information is available, Average Daily Traffic (ADT) can be used; g_i is the proportion of vehicles type i in the fleet; $\Delta t_i(T)$ corresponds to the time interval during which flows can affect the stability of vehicles type i during the flood with return period T.

Time interval $\Delta t_i(T)$ depended on the vehicle type because hazard was defined for the S_i of the flood peak and instability could take place for smaller flows. However, this time interval also depended on drivers' behaviour. The present methodology contemplated two different drivers' behaviours: (i) drivers did not decide to stop before crossing during floods in any case; (ii) for safety reasons, drivers decided to stop driving through the flooded area when the water depth exceeded a given value, which was called a limit water depth, and would not cross the stream crossing during the rest of the flood (the resulting value was lower than the previous one and in accordance with this limit water depth). One possible calculation appears in more detail in the case study.

To calculate risk, it is necessary to express vulnerability according to hazard. And for the latter an instrumental function is required, which can be called the exposure function of vehicles type i, $N_i(s_i)$ and was obtained by combining hazard and exposure, as depicted in Figure 2. This figure shows that, as previously indicated, a vehicle instability index S_i corresponded to each event with a given probability (Hazard, panel A, which is the resulting C in Figure 1) and a number of vehicles N_i driving through the stream crossing (Exposure, panel B). In this way, it was possible to relate the vehicle instability index S_i to the corresponding numbers of vehicles N_i, which gave a similar graph to that found in panel C with the vehicles' exposure function.

3.2.2 | Susceptibility

Susceptibility in the methodology herein presented was established by a damage function for each vehicle type i, $D_i(s_i)$, which is defined using vehicle instability index S_i values. It was assumed that the damage caused to vehicles was in accordance with their stability, and in such a way that when vehicles became unstable ($S_i < 0$ or $S_i \geq 1$), damage was complete ($D = 1$), but when vehicles remained stable ($0 \leq S_i < 1$), damage was null ($D = 0$). A graphical representation of this function is depicted in Figure 3, panel A.

Finally, the vulnerability for vehicles type i, $V_i(s_i)$, was obtained by combining the $D_i(s_i)$ damage and exposure $N_i(s_i)$ functions, as shown in Figure 3. This vulnerability was measured as the number of destabilised vehicles as a function of the vehicle instability index S_i.
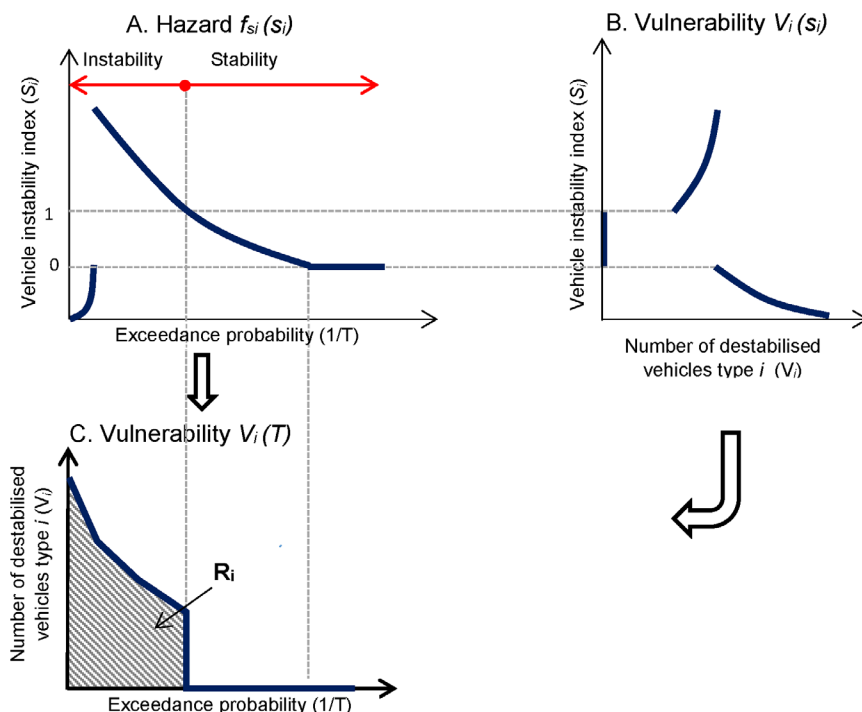

FIGURE 4   Outline of the process to calculate the instability risk for flooding vehicles type i in a stream crossing

3.3 | Vehicle instability risk

The instability risk was calculated by replacing the expressions obtained for both the hazard and vulnerability of the vehicles driving through a stream crossing in Equation 4). Figure 4 outlines the procedure that must be set up to calculate the instability risk for flooding of vehicles type i in stream crossings. Panel A (which is the resulting panel C of the Figure 1) corresponds to the instability hazard, which was obtained following the procedure described in Section 3.1. Panel B (which is the resulting panel C of the Figure 2) corresponds to vulnerability, which was obtained as set out in Section 3.2. When hazard was combined with vulnerability, for each flooding event with a given exceedance probability, a corresponding number of vehicles N_i would lose their stability in stream crossings (Figure 4, panel C). The instability risk for vehicles type i, R_i, corresponded to the integral of this function.

As Equation 4) only contemplates one type of vehicles, the total risk was obtained when using the summation of the partial risk obtained for the K types of vehicles with which the fleet was represented. So, the total risk would be:

$$R = \sum_{i=1}^{K} R_i = \sum_{i=1}^{K} \int_{0}^{\infty} V_i(s) f_{S_i}(s) ds \qquad (6)$$

In practice, it is not possible to calculate and obtain the integral of Equation (6) as we did not work with analytical functions and had a limited M number of flood maps. A discrete approach could be as follows:

$$R = \sum_{i=1}^{K} \left\{ \left[\sum_{j=0}^{M-1} \frac{V_i(s_{i,j}) + V_i(s_{i,j+1})}{2} \left(\frac{1}{T_j} - \frac{1}{T_{j+1}} \right) \right] + V_i(s_{i,M}) \left(\frac{1}{T_M} \right) \right\} \qquad (7)$$

where j corresponds to the number of the order of flood maps, which varied from 0 to T_{min} up to M for T_{max}, with T_{min} being the lowest return period from which vehicles would start being affected; T_{max} is the longest return period with an available flood hazard map; $V_i(S_{i,j})$ corresponds to the vulnerability of vehicle type i for a vehicle instability index S_i during the flood with return period T_j.

The last term in Equation (7) corresponds to the residual risk for longer return period events than T_{max}, for which the same vulnerability as T_{max} was assumed.

4 | APPLICATION TO A CASE STUDY

The developed methodology was employed to determine the vehicle instability risk for flooding in the stream crossings found in the Godelleta municipality, which lies very close to the Spanish Mediterranean coastline (Figure 5). This allowed the applicability of the methodology to be determined. For the case study, it also permitted the influence of both drivers' behaviour and the degree of obstruction of vented fords on the results to be analysed.
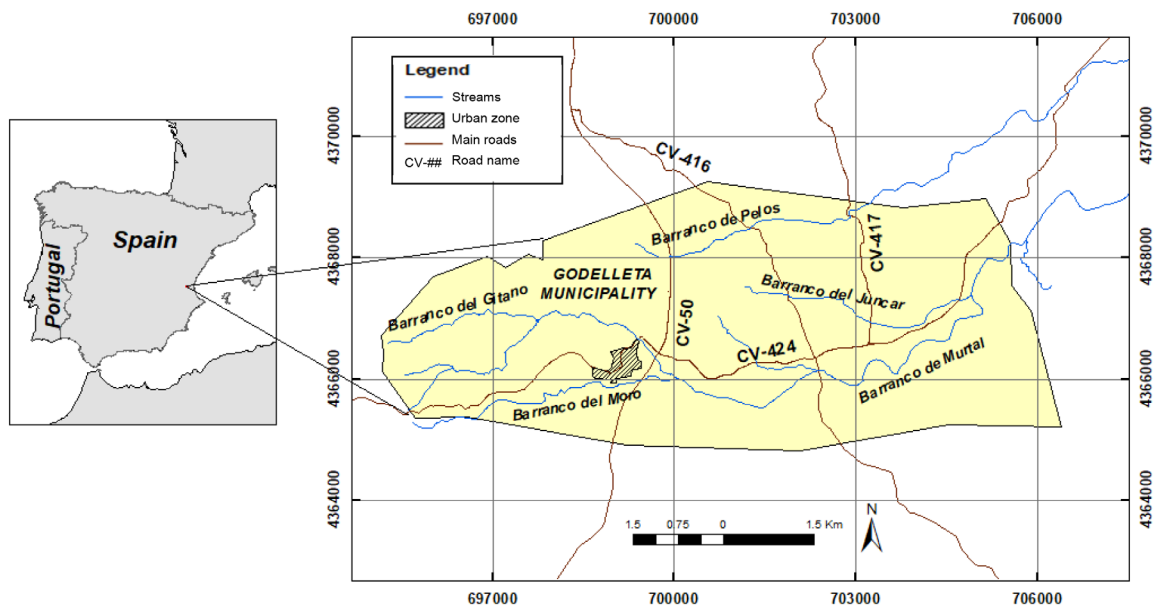

FIGURE 5 Location of the Godelleta municipality, ravines, main roads and its built-up area
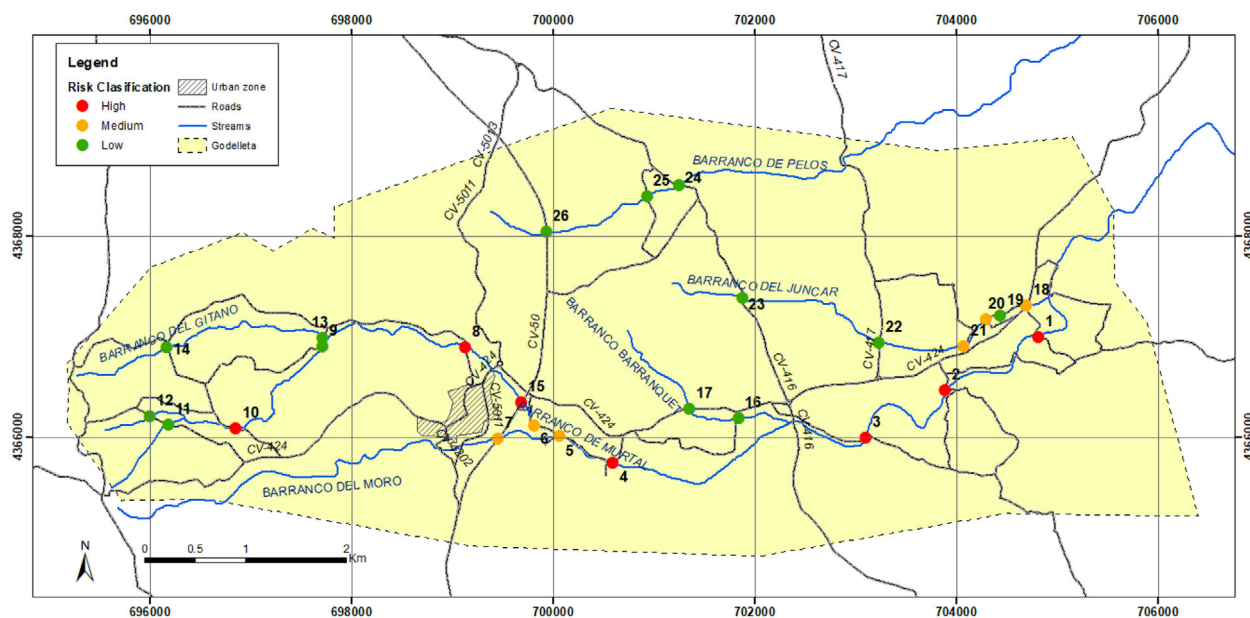
FIGURE 6 Vehicle instability risk due to floods in the stream crossings in the Godelleta municipality

4.1 | Characterisation of the study area

The Godelleta municipality covers 37.5 km², has a population of 3441 inhabitants, is relatively flat with gentle slopes and a mean height of 266 masl. Its climate is semi-arid Mediterranean with very variable mean precipitation figures around 450 mm, and rainfall concentrates in spring and autumn months.

The Godelleta municipality lies in the middle of the Rambla del Poyo Basin, which is an intermittent 43.5 kilometre-long current that has its maximum altitude at 1023 masl and flows into the Albufera coastal lagoon at sea level. The basin covers 430 km². Its slope varies between 16% at the highest point and 2% in the lowest part, where flash flooding occasionally occurs in autumn months (Salazar, 2013). This municipality has a drainage network made up of several ephemeral water currents that flow westerly–easterly of a torrential nature, with maximum flows in spring and autumn (Terrasa et al., 2018).

This municipality's road network is relatively dense and formed by regional and local roads in good condition. Regional roads include roads CV-50, CV-416, CV-417 and CV-424 (Figure 4). The last three roads are B-roads (single lane for each direction) that are relatively narrow with no verges. Road CV-50 is also a B-road, but has ample verges on both sides.

The intersection between the drainage network and the road network involves 32 stream crossings. The vehicles driving through these crossings via these roads would be at risk for instability due to floods that could occur in ravines. Of these 32 stream crossings,

8 correspond to fords, 18 to vented fords and 6 to bridges. In this paper, the risk in the stream crossings corresponding to fords and vented fords was calculated because the drainage capacity of these bridges corresponds to very little exceedance probabilities and, therefore, the risk of vehicles being dragged away is negligible. Figure 6 presents the location of the analysed fords and vented fords.

4.2 | Characterisation and exposure of the vehicles driving through the study area

The characterisation of the vehicles found in the study area was done using the official 2018 data reported by the Spanish Association of Manufacturers of Automobiles and Lorries (ANFAC, 2018). The analysis of these data established that the vehicles fleet driving around the Godelleta municipality can be suitably described by these vehicle types: (i) small cars; (ii) compact cars; (iii) small SUVs; and (iv) medium-sized SUVs and larger vehicles. These vehicle types are represented by the vehicles found in Table 1 of the work by Bocanegra and Francés (2021).

The traffic data for roads CV-416, CV-417 and CV-424 were taken from the official traffic levels of the Diputació de Valencia (2018). The road traffic data for road CV-50 were acquired from the information reported by the Generalitat Valenciana (2019). The ADT (number of vehicles/day), reported by these institutions for the sites of interest for this study, was as follows: (i) CV-50: 5141; (ii) CV-416: 380; (iii) CV-417: 484; (iv) CV-424: 7369. No official traffic levels data were available for local roads.

TABLE 1 Vehicle instability hazard index (only for one return period) and total risk due to floods in the stream crossings of the Godelleta municipality

Stream crossings	Stream	Stream crossings with culvert	Traffic flow q (cars/h)	Flood duration (h)	50 years flood return period Discharge (m³/s)	Hazard index S_i Vehicle type Small cars	Compacts	Small SUVs	Med. SUVs	Instability risk (cars/year) Actual	Potential
1	Del Murtal	Yes	45.32	6.2	73.71	−0.42	−0.43	−0.45	−0.52	0.35	4.67
2		Yes	0.50	6.1	70.80	−0.14	−0.14	−0.14	−0.15	0.21	1.85
3		Yes	1.51	6.0	67.68	−0.26	−0.25	−0.26	−0.28	0.22	3.80
4		No	1.01	5.5	53.55	−0.86	−0.82	−0.86	−0.90	1.12	2.37
5		Yes	1.51	5.3	47.71	−0.22	−0.21	−0.22	−0.23	0.11	2.99
6		No	0.21	4.7	33.13	−0.13	−0.12	−0.13	−0.13	0.11	0.46
7		Yes	214.21	4.7	32.96	0.00	0.00	0.00	0.00	0.16	2.21
8		Yes	4.03	4.4	25.72	−0.21	−0.20	−0.21	−0.23	0.65	2.13
9		Yes	6.04	3.8	13.41	−0.22	−0.21	−0.22	−0.24	0.08	1.56
10		No	3.02	3.5	8.58	−74.99	26.73	7.79	3.80	0.39	0.48
11		No	0.33	3.0	2.87	−0.72	−0.89	−1.14	−4.20	0.01	0.02
12	Del Borreguero	Yes	0.33	3.0	3.02	0.00	0.00	0.00	0.00	$<10^{-4}$	$<10^{-4}$
13	Del Gitano	Yes	6.04	3.6	11.33	−0.56	−0.69	−0.88	−3.23	0.02	0.29
14		No	0.32	3.1	3.84	10.13	1.58	0.58	0.31	1×10^{-3}	0.01
15	Del Moro	Yes	214.21	4.2	21.73	0.00	0.00	0.00	0.00	0.20	1.15
16	Barranquet	Yes	0.28	3.6	10.36	0.11	0.09	0.01	0.00	2×10^{-4}	0.004
17		Yes	96.42	3.4	7.84	0.00	0.00	0.00	0.00	5×10^{-4}	0.001
18	Del Juncar	Yes	307.04	3.8	14.08	0.03	0.03	0.00	0.00	0.18	3.71
19		Yes	12.08	3.8	13.68	0.50	0.33	0.14	0.08	0.04	0.25
20		No	0.53	3.8	13.52	−0.36	−0.36	−0.37	−0.40	0.18	0.52
21		No	0.27	3.7	12.84	−0.02	−0.02	−0.02	−0.02	0.12	0.42
22		Yes	20.17	3.6	10.58	0.05	0.05	0.00	0.00	0.02	0.20
23		Yes	15.83	3.1	4.16	0.00	0.00	0.00	0.00	3×10^{-4}	3×10^{-4}
24	De Pelos	Yes	15.83	3.7	13.15	0.51	0.33	0.14	0.09	0.04	0.33
25		No	0.28	3.5	9.86	−0.55	−0.60	−0.65	−0.93	0.003	0.04
26		Yes	271.75	3.2	5.86	0.00	0.00	0.00	0.00	$<10^{-4}$	$<10^{-4}$

Note: The locations of the intersection points are found in Figure 5.

4.3 | Vehicle instability hazard

The flows corresponding to the floods in the ravines found in the study area were determined by interpolation techniques using existing flow data about Rambla del Poyo at several basin points for return periods of 1, 2, 5, 10, 25, 50, 100 and 500 years. The flows of all the stream crossings were interpolated using the expression proposed by Leopold et al. (1964), which allows floods with drainage areas and their corresponding return periods to be related:

$$Q_T \propto A_d{}^b \, T \quad (8)$$

where Q_T is the peakflow quantile, A_d is the drainage area in each stream crossing, b is an exponent which, according to Leopold et al. (1964), varies between 0.65 and 0.80, and T is the return period. With the Rambla del Poyo fit, the determination coefficient significantly increased if an exponent was included in the return period. The final outcome used to estimate the flow quantiles at any point of Rambla del Poyo (including the ravines in the Godelleta municipality) was this expression:

$$Q_T = 0.4929 \, A_d^{0.75} \, T^{0.6512} \quad (9)$$

where Q_T is given in m³/s, A_d in km² and T in years.

The water levels and velocities corresponding to each analysed flow at the sites of interest were calculated assuming unidimensional stationary flow in a river section that included the stream crossing. These modellings were done with the HEC-RAS software, a widely used in hydraulic engineering. In these modellings, the geometric representation of the riverbed was performed with the cross-sections obtained from the digital elevations model of the Spanish National Centre of Geographic Information of Spain for all Spanish territory (Centro Nacional de Información Geográfica de España, 2019, http://centrodedescargas.cnig.es/Centro Descargas/index.jsp#, last consulted in September 2019) and based on the field trips of August 2019. The geometry of the fords and vented fords was obtained during field trips.

With the results obtained with the performed modelling, and having implemented the procedure described in Section 3.1, instability indices S_i were calculated for each analysed vehicle type for the different defined return periods. These indices were calculated by assuming that vehicles were completely watertight and lay perpendicularly to the flow. Table 1 presents the instability indices S_i obtained for the different vehicle types in all the stream crossings, but only for the flow with the 50-year return period.

The obtained vehicle instability indices S_i indicated that the flows with return periods that equalled or exceeded 50 years posed a high risk for the vehicles driving through stream crossings because, for a flood with a 50-year return period, the vehicle stability of roughly 55% of the vehicles would be lost. This percentage also had a significant value for the flood with a 25-year return period because it came close to 45%, and it almost reached 90% for a 500-year return period.

4.4 | Vulnerability

Vulnerability was calculated by combining susceptibility and vehicles' exposure to floods. Susceptibility was established through the damage function defined in Section 3.2.1. The damage function values either equalled 1 for flooding events in which vehicle instability index S_i had negative values (destabilisation due to floating) or exceeded or equalled 1 (destabilisation due to dragging). When vehicle instability index S_i had positive values below 1, the damage function equalled 0.

The exposure function was determined by bearing in mind that, according to that established in Section 3.2.2, for a given flooding event, the number of vehicles type i exposed to floods, N_i would correspond to the mean number of cars i that would drive through the flooded site during time interval Δt_i when the conditions leading to vehicle instability would take place. To know the duration of this time interval, we calculated the flood duration and times when the flow hydrodynamic conditions that would cause loss of vehicle stability would start and stop.

The flood duration time in the studied ravines was calculated by summing the duration time of rainfall events and the concentration time in each basin. The rainfall duration time was obtained from subtracting the concentration time for Rambla del Poyo from its mean flood duration time. According to Salazar (2013), the mean flood duration of Rambla del Poyo approximately equalled 12 h in the hydrometric station called Rambla del Poyo, where the drainage area equalled 184 km².

The concentration time, t_c, of both the Rambla del Poyo Basin and ravines was calculated by the following expression proposed by the Generalitat Valenciana (2018):

$$t_c = 0.7073 \, A_d^{0.4963} \quad (10)$$

Table 1 presents the flood duration times of the ravines found in the study area, which were obtained by

summing the rainfall duration time and the concentration time up to each stream crossing.

The water levels and flow velocities at which the analysed vehicle types would destabilise, and the time interval Δt_i during which stability would be lost in each flooding event, were determined by the results obtained with the hydrodynamic models developed for the stream crossings and the calculated vehicle instability indices S_i. Time interval Δt_i was calculated by contemplating the two possible drivers' behaviours set out in Section 3.2.2. For calculating under the condition for which it was assumed that drivers would decide to stop at a given time during the flood, a limit water depth equal to 0.3 m was adopted to interrupt the vehicle traffic (Shand et al., 2011; Pyatkova et al., 2015; Yin et al., 2016; Pregnolato et al., 2017).

The number of vehicles type i exposed to floods, N_i, was calculated by multiplying the vehicle traffic flow, q, by the proportion, g_i, of vehicles type i in the fleet, by the time interval, Δt_i, during which the conditions that would result in vehicle instability taking place. If official traffic levels data were available for roads, these data were used. However, if they were not available for some roads, then the vehicle levels recorded during field trips were employed. Table 1 shows the hourly flow of vehicles in all the stream crossings.

The exposure function was obtained by relating the vehicle instability index S_i calculated for each flooding event to the corresponding number of exposed vehicles N_i.

Finally, vulnerability was calculated by multiplying the results obtained by the damage and exposure functions for each flooding event.

4.5 | Vehicle instability risk

The vehicle instability risk was calculated by implementing the procedure described in Section 3.3. The risk obtained by considering that drivers would stop when flow depth reached the limit water depth was called actual risk, while that obtained by contemplating that drivers would not stop at any time was called potential risk. Table 1 offers the values obtained for the actual/ potential risks. Figure 6 graphically represents the actual risk; for graphical representation purposes only, this risk was subjectively classified as high for the values that equalled or exceeded 0.2 vehicles/year, medium when ranging between 0.1 and below 0.2 vehicles/year, and low if below 0.1 vehicles/year.

The analysis of the results concluded that the actual vehicle instability risk in the stream crossings in the Godelleta municipality was high for 27% of the existing intersections, medium for 23% of these stream crossings and low for the remaining 50%.

When analysing the results obtained by considering that vehicle traffic would continue moving throughout flood duration (potential risk), we observed that the values would be two-fold higher than those obtained after considering that vehicle traffic would cease at a given time. Accordingly, 69.2% of the stream crossings would obtain values above 0.2 vehicles/year and only 26.9% of the stream crossings would have values below 0.1 vehicles/year.

It is highlighted that most of the El Murtal Ravine stream crossings were at risk for vehicle instability. This risk can be considered medium or high, explained by this ravine having the biggest drainage area and greater flows inland of the Godelleta municipality. This condition coincides with the conclusion drawn by Versini et al. (2010), who evaluated the susceptibility of roads to flash floods in a sector of France. These authors found that the basin's area size upstream of the stream crossing was a very important factor for predicting floods in this sector.

It is noteworthy that the instability risk for the vehicles on roads with low traffic levels could be the same instability risk as those vehicles on roads with heavy traffic levels, as in points 6 and 7, which corresponded to the intersections of the El Murtal Ravine with the local road and road CV-50 with heavy traffic. These two stream crossings are separated from one another by approximately 600 m, with risk values equalling 0.11 and 0.16 vehicles/year, respectively. This was because, despite road CV-50 presenting very heavy traffic, vehicles would only be affected by floods with a 500-year return period. Although the traffic levels on the local road are much lower, vehicles would be affected by the floods corresponding to a 2-year return period.

According to the Generalitat Valenciana (2018), the diameter of the vented fords with circular culverts must be no less than 1.0 m to avoid obstructions caused by materials being dragged by flows. For the purpose of analysing the most unfavourable scenario possible, this analysis determined the vehicle instability risk by assuming a 0.3 m limit water depth and considering that the 10 vented fords with circular culverts whose diameters were less than 1.0 m, or presented equivalent geometries, were completely obstructed when flooding took place. Table 2 offers the results of this analysis. One conclusion was made according to this information: in all cases, the instability risk increased when culverts were obstructed or, in some cases, this increment could even surpass 100%. This shows the importance of employing vented fords of suitable dimensions and adequate maintenance to minimise the possibility of the vehicle instability risk increasing.

TABLE 2 Vehicle instability risk by taking a limit water depth of 0.3 m and vented fords with circular vents and a diameter less than 1.0 m, or equivalent geometries, being unblocked or completely obstructed

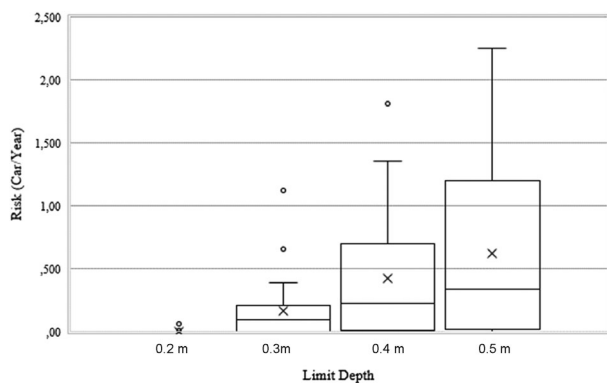| | Vehicle instability risk (vehicles/year) | | | | | | | | | |
| | Vented Ford | | | | | | | | | |
Degree of vented ford obstruction	2	3	5	8	9	12	13	19	22	23
Unblocked	0.21	0.22	0.11	0.65	0.08	2×10^{-6}	0.02	0.035	0.017	0.0003
Completely obstructed	0.39	0.47	0.13	0.87	0.26	3×10^{-6}	0.07	0.042	0.018	0.0004

FIGURE 7 Number of vehicles at instability risk in the Godelleta municipality by considering different water depth values from which vehicle traffic could cease

4.6 | Influence of the limit water depth

The number of vehicles at risk for instability due to floods is directly related to the limit water depth, and the risk becomes higher when drivers take poorly conservative attitudes. Nonetheless, determining this water depth is clearly associated with uncertainty because a large number of parameters influence decision making. For this reason, the effect of variation in this water depth was studied on the values of the at-risk vehicles, for which risk was determined by assuming water depths of 0.2, 0.4 and 0.5 m, where 0.3 m was the value taken while following the methodology. Figure 7 offers the obtained results.

Our results indicated that the instability risk was extremely sensitive to the water depth from which vehicle traffic stopped. When vehicle traffic was interrupted by a 0.2 m water depth, the risk equalled zero for almost all the stream crossings. This behaviour did not include the fords corresponding to points 6 and 10, where the risk values were 0.01 and 0.06 vehicles/year, respectively. When taking limit water depth values of 0.4 and 0.5 m, we found that, in relation to the values obtained when following the methodology, the mean risk value increased by almost 250% and 400%, while the maximum values rose by almost 50% and 100%, respectively. As the

minimum risk value did not undergo any major modifications when the limit water depth varied by between 0.2 and 0.5 m, as in point 12 where vehicles would only be affected by flows with return periods exceeding 500 years.

The range of variation of the instability risk values for the different stream crossings widened as the limit water depth value increased. The interquartile range equalled 0 m when considering a limit water depth of 0.20 m. The interquartile range value was 0.20 m for a limit water depth of 0.3 m. It increased to 0.63 m with a 0.40 m limit water depth and to 1.18 m with one of 0.50 m.

5 | CONCLUSIONS

The present article describes the a statistically sound methodology that allows instability risks due to floods to be estimated for vehicles driving through stream crossings, which may correspond to fords, vented fords or bridges. With bridges, this methodology can be used for hypothesising that bridge structures would not fail during floods. The calculated risk corresponded to the annual mean number of vehicles that would float or be dragged by the flow.

With this methodology, instability risk was calculated by combining hazard and vulnerability. To determine hazard, the stability function of partially submerged vehicles, the geometric characteristics of vehicles, the hydrodynamic characteristics of floods (water depths and velocities) and their exceedance probabilities were employed. Vulnerability was determined by combining exposure and susceptibility, which are respectively established with the exposure and damage function. Finally, risk was calculated by the discrete solution of the statistical integral of the product of hazard by vulnerability.

The developed methodology was applied to the Godelleta municipality, and found that roughly one quarter of the stream crossings in this study area presented a relatively high vehicle instability risk due to floods, because it exceeded 0.2 vehicles/year. Conversely, the

risk of approximately half these stream crossings could be considered relatively low, because it did not exceed 0.1 vehicles/year.

The number of vehicles at risk for instability due to floods proved extremely sensitive to the magnitude of the limit water depth from which drivers would decide to stop driving through flooded zones. Therefore, determining a safe limit water depth, that is, one associated with a low risk level, can help to encourage drivers' good behaviour. Also, this risk can significantly increase according to the extent that vented fords are obstructed. To avoid this risk increasing, periodically performing maintenance tasks should minimise this possibility.

The methodology developed in the present study can be implemented by the organisations responsible for urban planning and road traffic management to identify critical stream crossings in order to contribute to vehicle stability and to take measures that allow the potential negative impact of floods to lower. Some of the measures that can be taken, and would contribute to cushion the impact of floods, would be to, for instance, suitably maintain fords and vented fords, fit new culverts or increase the size of existing ones. This would allow the lowest return period value from which vehicles would be affected to increase, namely T_{min}. Drivers' good behaviour can be encouraged by informing that they must stop when the flow depth in the stream crossing reaches a certain limit water depth, which might allow the value of the time interval during which flow could affect vehicle stability, namely $\Delta t_i(T)$, to lower.

ACKNOWLEDGEMENT

DATA AVAILABILITY STATEMENT

The data that support the findings of this study are openly available in Riunet, http://riunet.upv.es.

ORCID

Ricardo A. Bocanegra https://orcid.org/0000-0003-3768-7486
Félix Francés https://orcid.org/0000-0003-1173-4969

REFERENCES

ANFAC, Spanish Association of Truck and Automobile Manufacturers (2018). Asociación Española de Fabricantes de Automóviles y Camiones. Retrieved from http://www.anfac.com/estadisticas.action.

Arrighi, C., Alcérreca-Huerta, J., Oumeraci, H., & Castelli, F. (2015). Drag and lift contribution to the incipient motion of partly submerged flooded vehicles. Journal of Fluids and Structures, 57, 170–184. https://doi.org/10.1016/j.jfluidstructs.2015.06.010

Arrighi, C., Castelli, F., & Oumeraci, H. (2016). Effects of flow orientation on the onset of motion of flooded vehicles. In Proceedings of the 4th IAHR Europe Congress, Liege. CRC Press.

Bocanegra, R. A., & Francés, F. (2021). Assessing the risk of vehicle instability due to flooding. Journal of Flood Risk Management, 14, e12738. https://doi.org/10.1111/jfr3.12738.

Bocanegra, R. A., Vallés-Morán, F. J., & Francés, F. (2020). Review and analysis of vehicle stability models during floods and proposal for future improvements. Journal of Flood Risk Management, 13, e12551. https://doi.org/10.1111/jfr3.12551

Cal y Mayor, R., & Cárdenas, J. (2007). Ingeniería de tránsito fundamentos y aplicaciones (8th ed.). Alfaomega.

Centro Nacional de Información Geográfica de España (2019). Retrieved from http://centrodedescargas.cnig.es/CentroDescargas/index.jsp#.

Dawson, R. J., Gosling, S., Chapman, L., Darch, G., Watson, G., Powrie, W., Bell, S., Paulson, K., Hughes, P., Wood, R., Thompson, D., & Johns, D. (2016). Chapter 4: Infrastructure in UK Climate Change Risk Assessment 2017 (CCRA 2017). In Adaptation Sub-Committee (ASC) of the Committee on Climate Change. Climate Change Committee.

de Valencia, D. (2018). Libro de Aforos 2017. Área Carreteras Servicio de Seguridad Vial y Supervisión.

Drobot, S. D., Benight, C., & Gruntfestd, E. C. (2007). Risk factors for driving into flooded roads. Environmental Hazards, 7(3), 227–334. https://doi.org/10.1016/j.envhaz.2007.07.003

Fitzgerald, G., Du, W., Jamal, A., Clark, M., & Hou, X. (2010). Flood fatalities in contemporary Australia (1997–2008). Emergency Medicine Australasia, 22, 180–186. https://doi.org/10.1111/j.1742-6723.2010.01284.x

Fhola de S. Paulo. (2020). Com chuvas perto do triplo da média, MG tem 53 mortos em cinco dias. https://www1.folha.uol.com.br/cotidiano/2020/01/numero-de-mortos-em-decorrencia-das-chuvas-em-mg-sobe-para-50.shtml

Generalitat Valenciana (2018). Guía de aplicación del plan de acción territorial sobre prevención del riesgo de inundación en la Comunitat Valenciana (Patricova). Diputación de Valencia - Área de Carreteras.

Generalitat Valenciana. (2019). Tráfico de las carreteras gestionadas por la Consellería 2018 y 4 años anteriores. Consellería de Política Territorial, Obras Públicas y Movilidad.

Jones, J. A., Swanson, F. J., Wemple, B. C., & Snyder, K. U. (2000). Effects of roads on hydrology, geomorphology, and disturbance patches in stream networks. Conservation Biology, 14, 76–85. https://doi.org/10.1046/j.1523-1739.2000.99083.x

Kalantari, Z., Santos, F. C. S., Koutsouris, A. J., Ahlmer, A. K., Cerdà, A., & Destouni, G. (2019). Assessing flood probability for transportation infrastructure based on catchment characteristics, sediment connectivity and remotely sensed soil moisture. Science of the Total Environment, 661, 393–406. https://doi.org/10.1016/j.scitotenv.2019.01.009

Leopold, L. B., Wolman, G. M., & Miller, J. P. (1964). Fluvial processes in geomorphology. Dover.

Levante (2019). La gota fría deja 5 muertos, 3.500 evacuados y daños catastróficos en el sureste. https://www.levante-emv.

com/sucesos/2019/09/14/gota-fria-deja-5-muertos/1921561. html

Michielsen, A., Kalantari, Z., Lyon, S. W., & Liljegren, E. (2016). Predicting and communicating flood risk of transport infrastructure based on watershed characteristics. *Environmental Management*, *182*, 505–518. https://doi.org/10.1016/j.jenvman.2016.07.051

Molarius, R., Könönen, V., Leviäkangas, P., Zulkarnain, R. J., Hietajärvi, A. M., & Oiva, K. (2014). The extreme weather risk indicators (EWRI) for the European transport system. *Natural Hazards*, *72*, 189–210. https://doi.org/10.1007/s11069-013-0650-x

Oshikawa, H., & Komatsu, T. (2014). Study on the risk evaluation for a vehicular traffic in a flood situation. In *Proceedings of the 19th IAHR-APD congress*. Hanoi: Construction Publishing House.

Pregnolato, M., Ford, A., Wilkinson, S. M., & Dawson, R. J. (2017). The impact of flooding on road transport: A depth–disruption function. *Transportation Research Part D*, *55*, 67–81. https://doi.org/10.1016/j.trd.2017.06.020

Pyatkova, K., Chen, A.S., Djordjevic, S., Butler, D., Vojinović, Z., Abebe, Y.A., Hammond, M.J., (2015). Flood impacts on road transportation using microscopic traffic modelling technique. SUMO User Conference 2015 Proceedings, Berlin (Germany).

Prada, R., & Carolina, M. (2015). *Flood risk in road networks (English). Advances in probabilistic flood hazard assessment (CAPRA) technical notes*. World Bank Group. http://documents.worldbank.org/curated/en/953881468189843526/Flood-risk-in-road-networks

Salazar, S. (2013), Metodología para el análisis y la reducción del riesgo de inundaciones: Aplicación en la Rambla del Poyo (Valencia) usando medidas de "retención del agua en el territorio." Doctoral Thesis, Universidad Politécnica de Valencia. Riunet Institutional Repository.

Shand T., Cox R., Blacka M., Smith G. (2011). Australian Rainfall and Runoff (AR&R). *Appropriate safety criteria for vehicles*. Australian rainfall and runoff, revision project 10: Report Number: P10/S2/020, Sydney, Australia.

Suárez, P., Anderson, W., Mahal, V., & Lakshmanan, T. (2005). Impacts of flooding and climate change on urban transportation: A system wide performance assessment of the Boston Metro Area. *Transportation Research Part D*, *10*, 231–244. https://doi.org/10.1016/j.trd.2005.04.07

Terrasa S. O., Merino S. M., García E. M., Casado R. E., Pareja M. R., Quesada M. L., Vives R. N., Troyano G. J., Estevens M. E., Ruíz G. J., Barelles A. J., Gaja S. P. (2018). Plan general de ordenación urbana Informe de sostenibilidad ambiental, Godelleta.

UNISDR, (2009). *Terminología sobre reducción del riesgo de desastres. Estrategia para la reducción de desastres de las Naciones Unidas*. https://floodresilience.net/resources/item/terminologia-sobre-reduccion-del-riesgo-de-desastres

Versini, P. A., Gaume, E., & Andrieu, H. (2010). Assessment of the susceptibility of roads to flooding based on geographical information—Test in a flash flood prone area (the Gard region, France). *Natural Hazards and Earth System Sciences*, *10*, 793–803. https://doi.org/10.5194/nhess-10-793-2010

Wemple, B. C., Swanson, F. J., & Jones, J. A. (2001). Forest roads and geomorphic process interactions, Cascade Range, Oregon. *Earth Surface Processes and Landforms*, *26*, 191–204.

Yin, J., Yu, D., Yin, Z., Liu, M., & He, Q. (2016). Evaluating the impact and risk of pluvial flash flood on intra-urban road network: A case study in the city center of Shanghai, China. *Journal of Hydrology*, *537*, 138–145. https://doi.org/10.1016/j.jhydrol.2016.03.037